International Journal of Earth, Energy and Environmental Sciences
ISSN: 2517-942X
Vol:13, No:5, 2019

Critical Heights of Sloped Unsupported Trenches in Unsaturated Sand

Won Taek Oh, Adin Richard

***Abstract*—**Workers are often required to enter unsupported trenches during the construction process, which may present serious risks. Trench failures can result in death or damage to adjacent properties, therefore trenches should be excavated with extreme precaution. Excavation work is often done in unsaturated soils, where the critical height (i.e. maximum depth that can be excavated without failure) of unsupported trenches can be more reliably estimated by considering the influence of matric suction. In this study, coupled stress/pore-water pressure analyses are conducted to investigate the critical height of sloped unsupported trenches considering the influence of pore-water pressure redistribution caused by excavating. Four different wall slopes (1.5V:1H, 2V:1H, 3V:1H, and 90°) and a vertical trench with the top 0.3 m sloped 1:1 were considered in the analyses with multiple depths of the ground water table in a sand. For comparison, the critical heights were also estimated using the limit equilibrium method for the same excavation scenarios used in the coupled analyses.

***Keywords*—**Critical height, matric suction, unsaturated soil, unsupported trench.

I. Introduction

MOST engineering projects involving foundations, landfills, pipelines, storm drains, etc. are initiated with an excavation for infrastructure to be installed. Trenching is inherently dangerous due to the risk of cave-in, which may result in severe injury, death, or consequential damage to adjacent properties. Thousands of work-related deaths and injuries in the construction industry have been attributed to trench collapses. An average of 50 fatalities was reported each year from 1992 to 2007 in the U.S. alone [1].

In Canada, each province enforces strict regulations with respect to safe excavation practices in an attempt to prevent fatalities and serious injuries resulting from trench collapses. The regulations specify the maximum allowable height of an unsupported vertical trench (i.e. safe height), maximum sloping and benching angles, and the minimum distance from the trench for stockpiling excavated or backfill materials. Regardless of in situ field conditions, most Canadian provinces enforce safe height of 1.2 m except [2], [3] (i.e. 1.5 m).

Trench boxes are often a practical solution in protecting workers since they allow them to safely access the work space. However, typical trench boxes are eight meters in length and weigh multiple tons. Hence, the process of lifting a box, setting it in place, and repositioning it when necessary can be very time consuming. They also create an obstacle for the workers and the equipment that are used for setting infrastructure since lost production time results in lost profit, making it desirable to excavate and work in unsupported trenches whenever possible. However, unsupported trenches risk collapsing and therefore must be designed and excavated with extreme precaution, especially when workers are required to enter the trench.

The critical height (i.e. maximum depth of a trench that can be excavated without failure) is the most important design consideration for ensuring the stability of unsupported trenches. Many construction projects involve trenching and setting infrastructure in the vadose zone; thus, the critical height of unsupported trenches should be determined by extending the mechanics of unsaturated soils. Trench stability is mainly governed by the matric suction distribution between the soil surface and the ground water table [4]–[6]. In the other words, adhering to a universal safe height suggested by provincial regulations may not be a reasonable approach in geotechnical engineering practice, because in situ field conditions are not considered.

In the present study, an attempt was made to investigate the influence of excavation rate on the critical height of various sloped unsupported trenches in an unsaturated sand through coupled stress/pore-water pressure analysis using the geotechnical modelling software, SIGMA/W and SLOPE/W (GeoStudio 2016, GeoSlope Ltd. Inc.). Critical heights estimated for different excavation rate were also compared with those from the Limit Equilibrium method (i.e. Morgenstern-Price method).

II. Trench Failure Modes and Mechanism

Changes in pore-water pressure, surface loading, and vibration are the most predominant causes of trench instability, as in Fig. 1 [7]. The base and walls of a trench experience elastic rebound immediately after excavating due to the relief of confining pressures. This causes a decrease in pore-water pressure, thus increasing shear strength of the soil. Hence, a trench may appear stable immediately after excavating. However, the trench destabilizes over time as the equilibrium condition with respect to pore-water pressure within the soil nearby the trench base and walls is achieved with the dissipation of negative excess pore-water pressure. Rainfall infiltration, development of cracks, and a rising ground water table can further increase pore-water pressure and accelerate a trench failure. Thus, the risk of trench collapse increases as exposure time to the atmosphere

W. T. Oh is with the Department of Civil Engineering, University of New Brunswick, Fredericton, NB, E3B 5A3 Canada (e-mail: woh@unb.ca).

A. Richard was with the Department of Civil Engineering, University of New Brunswick, Fredericton, NB, Canada. He is now with BGC Engineering (e-mail: adin.richard9@gmail.com).

increases. Due to this reason, unsupported trenches should be backfilled as soon as the job is complete.

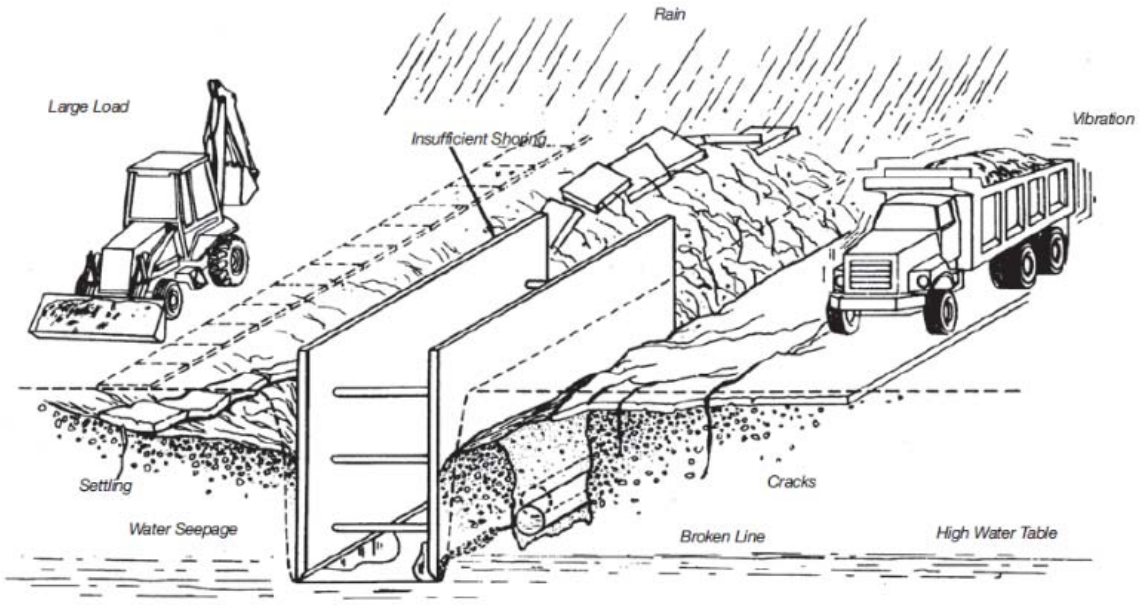

Fig. 1 Factors affecting trench stability [7]

Reference [3] categorizes the modes of trench collapse into four types, as in Fig. 2.

- Spoil pile slide (Fig. 2 (a)) - occurs when the excavated material is not placed far enough away from the edge of the excavation. A minimum distance of 0.6 m is recommended for every one-meter of excavation depth.
- Side wall shear (Fig. 2 (b)) - common to fissured or desiccated clay-type or alluvial soils that are exposed to drying.
- Slough-in (cave-in, Fig. 2 (c)) - common to previously excavated material, fill, and granular soils where the water table is above the base of the excavation, or where soils are organic or peat.
- Rotation (Fig. 2 (d)) - common in clay-type soils when excavation walls are too steep, or when moisture content increases rapidly.

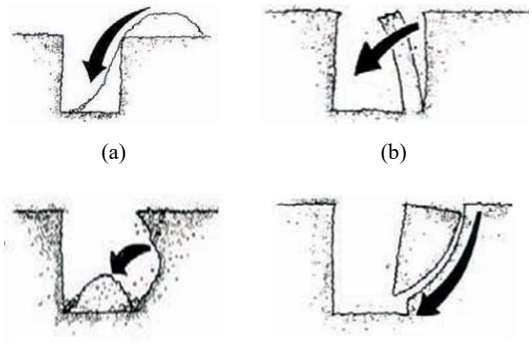

(a) (b)

(c) (d)

Fig. 2 Trench failure modes [3]

Reference [2] describes how rescue attempts may be more difficult and dangerous when the wall failure occurs sequentially, as in Fig. 3. In this case, failure is initiated at the base of the trench wall. Cracking near the ground surface and local failures in Zone 1 should raise alarms. This localized failure or movement leads to failure in Zone 2. Finally, the failure in Zone 3 occurs due to the self-weight of the soil. This failure sequence is a plausible explanation for why rescuers are sometimes trapped along with the first victim(s). Someone attempting to intervene and help uncover a victim when failure in Zone 3 has not yet occurred can put themselves at risk.

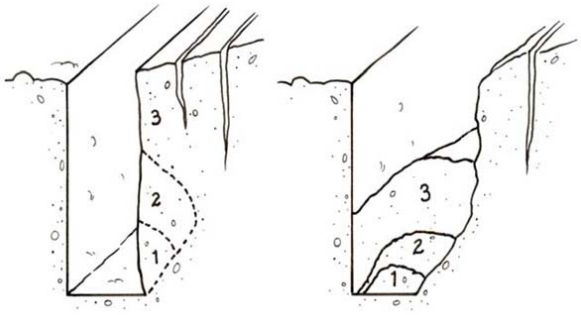

Fig. 3 Sequential trench failure [2]

III. Soil Properties

In this study, it was assumed that the trenches were excavated into Unimin 7030 sand (hereafter referred to as sand). Table I summarizes the properties of the sand used in the present study [8].

TABLE I
SOIL PROPERTIES OF UNIMIN 7030 SAND [8]

Properties	Value
Plasticity index, I_p	NP
Effective cohesion, c'	0
Effective internal friction angle, ϕ'	36.2°
Saturated unit weight, γ_{sat} (kN/m^3)	19.75
Saturated volumetric water content, θ_s	0.39
Void ratio, e	0.63
Specific gravity, G_s	2.65
Saturated hydraulic conductivity, k_s (m/s)	5×10^{-5}
Elastic modulus for saturated condition, E_s (kPa)	10,000

Grain-size distribution curve and SWCC (i.e. Soil-Water Characteristic Curve) of the sand are shown in Fig. 4 and Fig. 5, respectively. A best-fit analysis of the SWCC was carried out using (1) proposed by [9]. The variation of hydraulic conductivity with respect to matric suction (i.e. hydraulic conductivity function; Fig. 6) was estimated using the model proposed by [10], as in (2).

$$\theta = \theta_s \left[\frac{1}{\ln\left[e + \left((u_a - u_w)/a \right)^n \right]} \right]^m \quad (1)$$

where θ = volumetric water content, θ_s = volumetric water content for saturated condition, e = Napier's constant (i.e. 2.71828…), a (= 9.1638), m (= 16.544), and n (=4.8624) = fitting parameters

$$k(\psi) = k_s \frac{\sum_{i=j}^{N} \frac{\theta(e^y) - \theta(\psi)}{e^{y_i}} \theta'(e^{y_i})}{\sum_{i=1}^{N} \frac{\theta(e^y) - \theta_s}{e^{y_i}} \theta'(e^{y_i})} \quad (2)$$

where $k(\psi)$= the calculated conductivity for a specified water content or matric suction (m/s), k_s = the measured conductivity for saturated condition, (m/s), y = a dummy variable of integration representing the logarithm of negative pore-water pressure, i = the interval between the range of j to N, j = the least negative pore-water pressure to be described by the final function, N = the maximum negative pore-water pressure to be described by the final function, ψ = the suction corresponding to the j^{th} interval, and θ' = the first derivative of the equation.

IV. METHODOLOGIES

The critical heights were determined using two different approaches; finite element method (coupled stress/pore-water pressure analysis) and Limit Equilibrium method (Morgenstern-Price method). Analyses were conducted for 10 ground water table depths and four slopes as summarized in Table II.

The results showed that the estimated critical heights were not affected by the mesh size when finer than 0.25 m. 4-point integration was used for the quadrilateral elements, and 3-point integration was used for the triangular elements. A linear interpolation model was used for calculating stresses and deformations at the nodes. The left and right ends are restrained in the X-direction, and the base of the domain is restrained in both the X and Y directions (hollow triangles). Total head boundaries equal to the initial water table elevation were placed along the lateral extents of the soil region (i.e. solid circles). This allows the ground water table to fluctuate in response to excavating while maintaining constant hydraulic head along the extents of the domain.

TABLE II
SCENARIOS USED IN THE ANALYSES

Ground water table depth (m) (distance from the ground surface)	Trench Slopes
0, 0.3, 0.5, 0.7, 0.8, 0.9, 1.0, 1.2, 1.5, 2.0	90°, 3V:1H, 2V:1H, 1.5V:1H

A. Estimating the Critical Height using Coupled Analysis

Two codes, SIGMA/W and SLOPE/W, were jointly used to estimate the stability of unsupported trenches. The initial hydrostatic pore-water pressure distribution and gravity body loads were first established using 'In-Situ' feature in SIGMA/W. The meshes and boundary conditions are shown in Fig. 7. The meshes were created of 0.1 m × 0.25 m elements in the immediate surroundings of the excavation, and transitions to 1 m × 1 m elements along the extents of the domain. 'Quads & Triangles' mesh pattern was used to provide a smooth transition between areas of interest and to save on computation time. Mesh sizes were determined based on a mesh-convergence study conducted with different element lengths (1 m, 0.25 m, 0.1 m, and 0.05 m) and a 0.1 m thickness along the excavated surface.

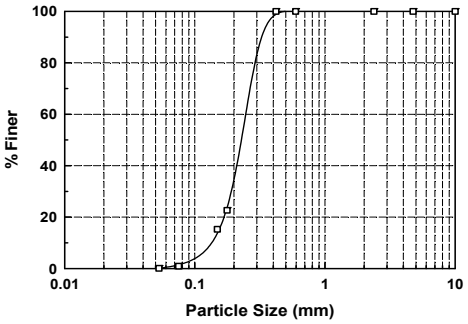

Fig. 4 Grain size distribution curve of Unimin 7030 sand

Excavations were simulated by deactivating regions in 0.1 m increments. This causes deformations and change in stresses in a soil, which leads to the redistribution of pore-water pressure. Hence, coupled stress/pore-water pressure analysis was carried out in SIGMA/W using effective stress parameters and the elastic-plastic constitutive model to simulate this scenario. The previous stage in the excavation was used as the parent analysis to the following, such that the stress changes and deformations caused by the previous excavations were compounded as the stages progressed.

Stability analyses were than conducted in SLOPE/W using SIGMA/stress method to determine the critical height based on the information from the SIGMA/W (i.e. deformation,

stress, and pore-water pressure) as the parent analysis. Two time steps between excavation stages (i.e. 10 sec and 1,000 sec) were considered in the stability analysis to investigate the variation of critical height for different excavation rates. The 'Entry and Exit' slip surface method was used for generating potential slip surfaces. The exit was specified as a point at the toe of trench, and the entry was defined as a range as wide as the excavation depth with a possible entry point every 10 mm along the ground surface. The critical height was defined as the excavation depth that showed Factor of Safety (FOS) = 1.0 (e.g. Fig. 8), or the depth prior to the excavation stage that showed FOS < 1.0 in the stability analysis.

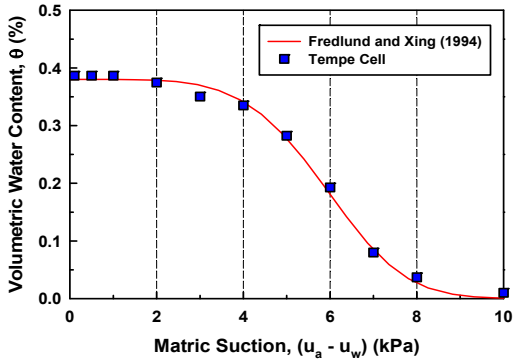

Fig. 5 Soil-Water Characteristic Curve of Unimin 7030 sand

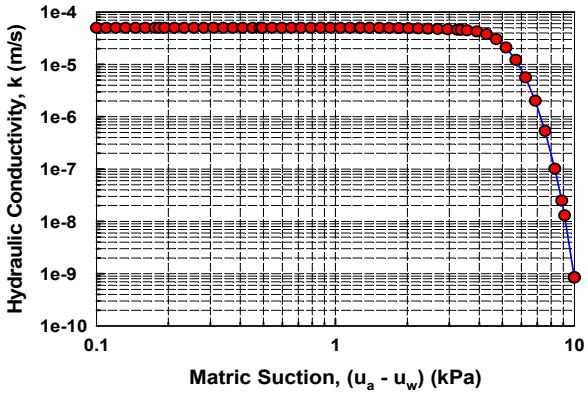

Fig. 6 Hydraulic conductivity function of Unimin 7030 sand used in the numerical analysis

B. Estimating the Critical Height using Limit Equilibrium Method

Stability analyses were also conducted using the Limit Equilibrium Method (LEM) for the same scenarios used in the coupled analyses to investigate the differences in the estimated critical heights. Fig. 9 shows the forces acting on a slice within an arbitrary slip surface and defines all geometric parameters [11]. Tension crack zone, lateral pressure due to water in tension cracks (A_R), external point load (D), and seismic loads were not considered in the analyses and are therefore omitted in calculating the FOS. Among various solutions to the LEM, the method proposed by [12] (hereafter referred to as M-P method) was used in the present study.

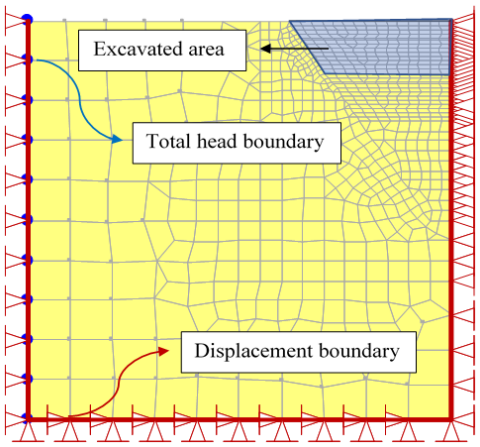

Fig. 7 Meshes and boundary conditions in SIGMA/W

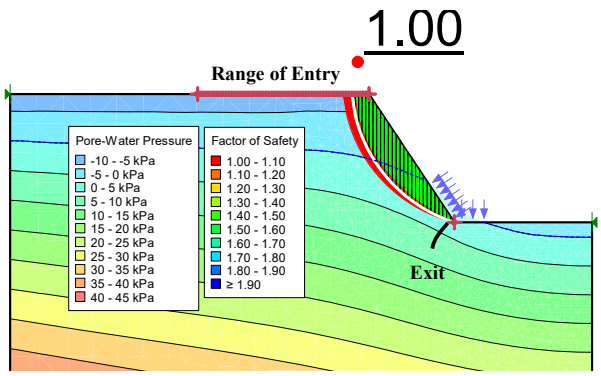

Fig. 8 Example of slope stability analysis using SIGMA/stress method in SLOPE/W (1.5H:1H)

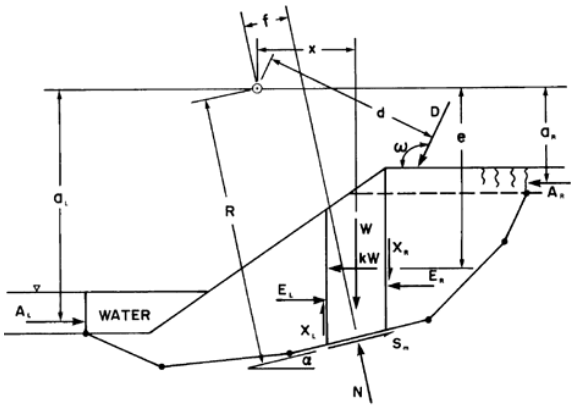

Fig. 9 Forces acting on a slice within an arbitrary slip surface [11]

The interslice forces are statically indeterminate with the LEM, therefore various solutions exist based on the assumptions made to solve for equilibrium. The M-P method accounts for both interslice normal and shear forces, assuming that the interslice shear force is a function of a scaling factor, an interslice force function, and the interslice normal force, as in (3). SLOPE/W computes the FOS in an unsaturated slope for moment and force equilibrium as shown in (4) and (5),

respectively. The normal force, N can be calculated using (6).

$$X = \lambda f(x) E \tag{3}$$

where X = interslice shear force per unit length, E = interslice normal force per unit length, λ = scaling factor, and $f(x)$ = specified interslice force function

$$FOS_m = \frac{\sum \left(c'\beta R + \left[\begin{matrix} N - u_w \beta \dfrac{\tan\phi^b}{\tan\phi'} \\ -u_a \beta \left(1 - \dfrac{\tan\phi^b}{\tan\phi'} \right) \end{matrix} \right] R \tan\phi' \right)}{\sum Wx - \sum Nf} \tag{4}$$

$$FOS_f = \frac{\sum \left(c'\beta \cos\alpha + \left[\begin{matrix} N - u_w \beta \dfrac{\tan\phi^b}{\tan\phi'} \\ -u_a \beta \left(1 - \dfrac{\tan\phi^b}{\tan\phi'} \right) \end{matrix} \right] \tan\phi' \cos\alpha \right)}{\sum N \sin\alpha} \tag{5}$$

$$N = \frac{W + (X_R - X_L) - \dfrac{\left[\begin{matrix} c'\beta \sin\alpha + u_a \beta \sin\alpha (\tan\phi' - \tan\phi^b) \\ + u_w \beta \sin\alpha \tan\phi^b \end{matrix} \right]}{FOS}}{\cos\alpha + \dfrac{\sin\alpha \tan\phi'}{FOS}} \tag{6}$$

where FOS_m = factor of safety for moment equilibrium, FOS_f = factor of safety for force equilibrium, N = slice base normal force per unit length ($FOS = FOS_m$ or FOS_f), W = total weight of a slice, c' = effective cohesion, ϕ' = effective internal friction angle, ϕ^b = internal friction angle indicating the rate of increase in shear strength with respect to a change in matric suction, u_a = pore-air pressure, u_w = pore-water pressure, X = vertical interslice shear forces, and E = horizontal interslice normal force

Determination of ϕ^b in above equations experimentally is time consuming and requires elaborate testing equipment. Due to this reason, several researchers proposed empirical or semi-empirical models that can be used to estimate the contribution of soil suction towards the shear strength of unsaturated soils. GeoStudio (2016) adopts (7) proposed by [13] to estimate the nonlinear variation of ϕ^b with respect to matric suction. SLOPE/W considers the variation of the unit weight of soil with respect to volumetric water content in the analysis based the SWCC, as in (8).

$$\phi^b = \frac{(\theta - \theta_r)}{(\theta_s - \theta_r)} \tan\phi' \tag{7}$$

where θ = volumetric water content, θ_s = volumetric water content for saturated condition, and θ_r = volumetric water content for residual condition

$$\gamma = \frac{G_s + \theta(1+e)}{1+e} \gamma_w \tag{8}$$

where e = void ratio, G_s = specific gravity, and γ_w = unit weight of water

V. Analysis of Results

A. Variation of FOS with Time in Coupled Analysis

Fig. 10 shows the variation of FOS with time for the case of a 1.5V:1H sloped excavation staged in 0.1 m increments up to 1.3 m with the initial ground water table at 0.7 m.

Detailed analyses results can be seen in Fig. 11 with the variation of deformation, pore-water pressure, and FOS for different time steps. The black arrows represent hydraulic velocity vectors, and the magnitude decreases with time as the pore-water pressure approaches equilibrium condition. There is sudden drop in FOS right after the excavation from 1.47 to 1.33. FOS remains almost constant thereafter until it starts rapidly decreasing around 500 sec after the excavation was initiated. This time step corresponds to the moment where the sand reaches an equilibrium condition with respect to pore-water pressure.

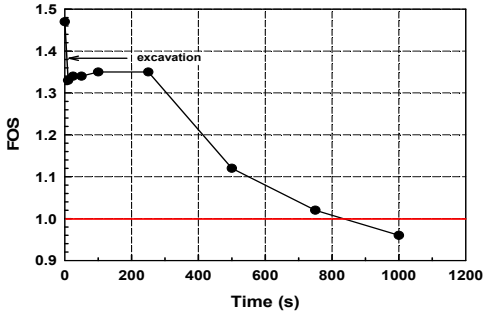

Fig. 10 FOS vs time for 1.3 m excavation stage (1.5V:1H) with initial ground water table at 0.7 m

As discussed previously, removing soil from the ground relieves overburden and confining pressures, which results in expansion of the soil adjacent to the excavated surface. Fig. 11 clearly shows that the deformations along the excavation face gradually increase over time. This sort of scenario may occur in practice if an excavation is made rapidly to a desired depth and left open for some period.

B. Comparison of Critical Height Estimated Using Different Approaches

In this section, critical heights estimated using two different approaches (i.e. coupled analysis and LEM) are compared. In coupled analysis, critical heights were estimated for two different time steps; namely, 10 sec and 1,000 sec. These time steps were chosen to simulate fast and slow excavation rates, respectively.

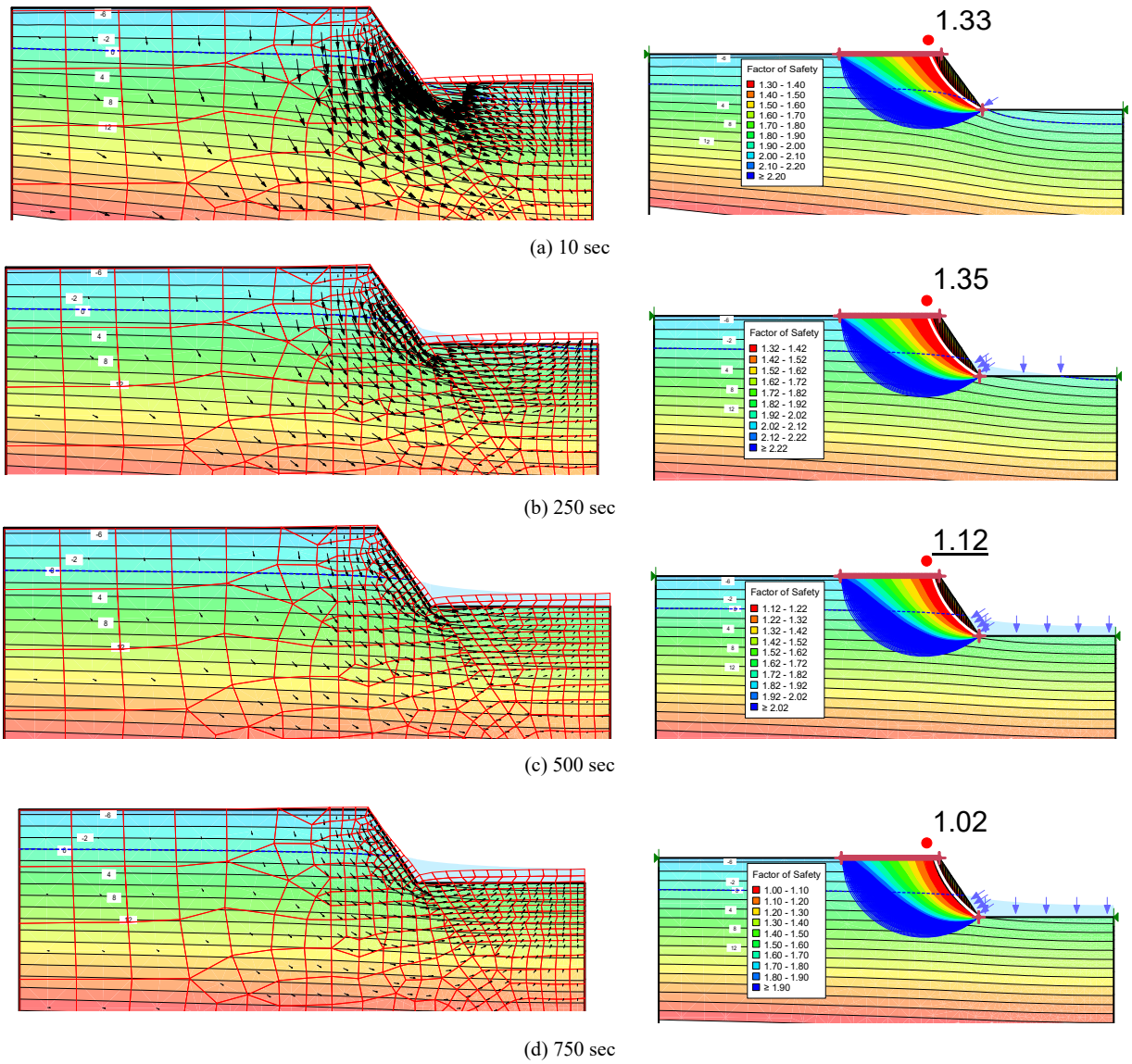

Fig. 11 Variation of deformation, PWP, and FOS with time for (a) 10 sec, (b) 250 sec, (c) 500 sec, and (d) 750 sec after 1.3 m excavation stage with initial ground water table at 0.7 m

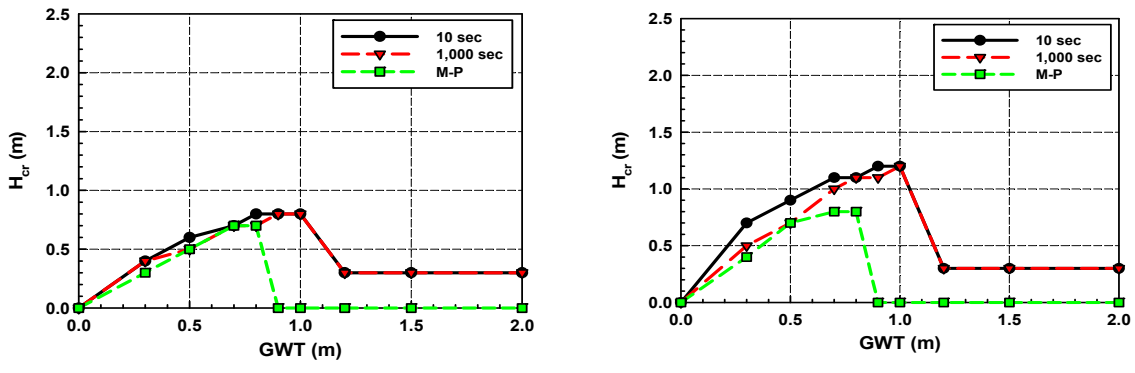

(a) (b)

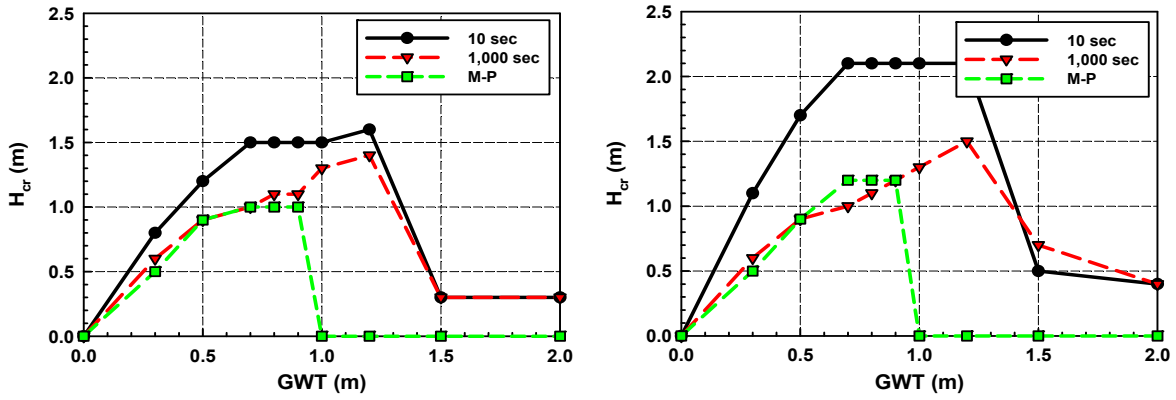

(c) (d)

Fig. 12 Variation of critical height for (a) 90°, (b) 3V:1H (c) 2V:1H and (d) 1.5V:1H slope in Unimin 7030 sand

Figs. 12 (a)-(d) show the critical heights for 90°, 3V:1H, 2V:1H, and 1.5V:1H excavation scenarios for different ground water table depths. The critical height decreases as the period between excavation stages increases (i.e. 10 sec to 1,000 sec time steps). This is because 10 sec time step excavations force the ground water table to continue dropping without giving enough time for the ground water table to rebound a significant amount. When a soil mass is removed from the ground, the soil within the proximity of the excavation experiences stress relief ranging from $K_0\sigma_z$ to σ_z in the horizontal and vertical directions, respectively (where σ_z is the vertical stress at a depth z, and K_0 is the coefficient of earth pressure at-rest). This indicates that the stress relief in the soil near the ground surface is minimal (or close to zero), and pore-water pressure changes are negligible. Therefore, as the slope of a trench decreases, more stress relief occurs along the face of the slopes and the (negative) change in pore-water pressure increases accordingly. Due to this reason, the difference in the critical heights between 10 sec and 1,000 sec time step increases with decreasing the slope of a trench. The largest difference in the critical heights between the coupled analysis (10 sec) and the M-P method is observed for the 1.5V:1H slope.

For coupled analyses with 1,000 sec time steps, most negative excess pore-water pressure dissipates and the critical heights show small discrepancies when compared with those from the M-P method when the ground water table depth is less than 1 m. When the ground water table is deeper than 1 m, the critical heights estimated with the M-P method are zero, but the coupled analyses show minimum values of 0.3 m. The main reason for this difference is related to the concentration of normal and shear stress in the toe area of a trench. This phenomenon leads to slightly higher FOS when estimated based on finite element stress compared to that of LEM. For this reason, a sloped trench can be excavated past the residual zone near the ground surface even when the ground water table is relatively deep (i.e. deeper than 1 m).

These results clearly show that the estimated critical height based on limit equilibrium conditions is more conservative compared with that of coupled finite element stress-based analyses. However, there are advantages of using finite element stress-based stability analyses such as i) displacement compatibility is satisfied and ii) the ground stresses are much closer to reality [14].

For a vertical trench, the critical height increases as the depth of the ground water table increases up to 0.8 m, and then declines sharply thereafter. As explained previously, a deep ground water table creates a residual suction zone near the ground surface, which results in a complete loss of total cohesion (Fig. 13). To further investigate this behavior, additional analyses were conducted for a vertical trench with the first 0.3 m of excavation sloped 1:1 (90**) as shown in Fig. 14. The results from the three methods for the 90** case are plotted in Fig. 15. For the M-P method, the maximum attainable critical height in a vertical trench was increased by 0.1 m and was sustained for an additional 0.1 m increase in the depth of the ground water table. For the coupled analyses, the 90*** case provides slightly higher critical heights with the ground water table 0.5 m and 1.5 m (see Fig. 12 (a) for comparison). Hence, it seems that benching or sloping the soil in the residual zone at 1:1 slope is not as effective as sloped trenching.

VI. Summary and Conclusions

Coupled stress/pore-water pressure and Limit Equilibrium methods (i.e. Morgenstern-Price) were used to investigate the influence of various slopes and matric suction distributions on the critical height of unsupported trenches in an unsaturated sand. The results from the current study are summarized as follow.

1) An unsupported trench can remain stable during certain period after excavation. However, the coupled analyses results showed that it may fail as pore-water pressure reaches equilibrium condition over time. Thus, it is more conservative using LEM assuming a hydrostatic pore-water pressure distribution when estimating the critical height.
2) Critical height can be almost doubled by flattening the slopes compared to a vertical excavation. The main advantage of flattening the slope is that a greater critical

height can be achieved even when residual suction is reached near the ground surface.

3) Cutting a soil in residual zone can slightly increase the critical height, lends credibility to Canadian provincial standards [7], saying that 1:1 slope is sufficient for most excavations where a vertical trench cannot be excavated to a significant depth. However, it may not be as effective as sloped trenches if the cutting is made at shallow depth from the ground surface.

It may not always be possible to provide a slope to the excavation in geotechnical engineering practice due to limited space. In this case, a combination of gently slope and cutting upper soil can be used effectively to achieve targeted critical heights, especially when the soil surface is within the residual suction zone.

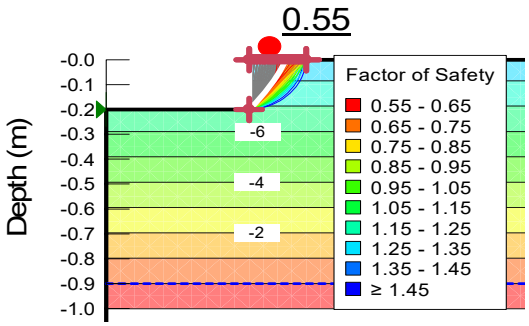

Fig. 13 Vertical trench with ground water table at 0.9 m (M-P method)

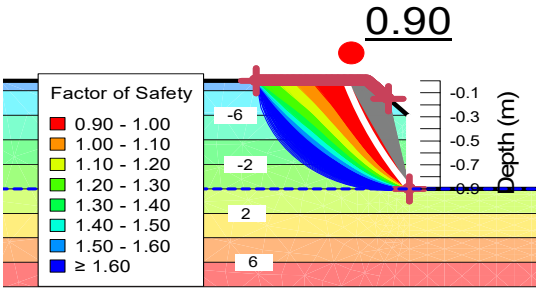

Fig. 14 Partially sloped (1:1) vertical trench with ground water table at 0.9 m (M-P method)

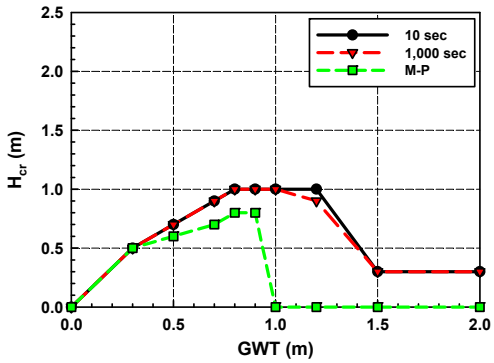

Fig. 15 Variation of the critical height for 90** slope in Unimin 7030 sand

References

[1] National Institute of Occupational Safety & Health (NIOSH), "Trenching and Excavation - Workplace Safety and Health Topic," US Department of Health and Human Services. 2007.

[2] Alberta, "Occupational Health & Safety Code - Explanation Guide," Occupational Health & Safety Division. 2009.

[3] Manitoba, "Guide for Excavation Work," Workplace Safety & Health Division. 2011.

[4] D. E. Pufahl, D. G. Fredlund, and H. Rahardjo, H.,"Lateral earth pressures in expansive clay soils," *Can. Geotech. J.*, vol. 20, no. 2, pp. 228–241. 1983.

[5] V. Whenham, M. D. Vos, C. Legrand, R. Charlier, J. Maertens, and J. – C. Verbrugge, "Influence of soil suction on trench stability," In Experimental Unsaturated Soil Mechanics, Springer Berlin Heidelberg, pp. 495–501. 2007.

[6] P. De Vita, A. C. Angrisani, and E. Di Clemente, "Engineering geological properties of the Phlegraean pozzolan soil (Campania region, Italy) and effect of the suction on the stability of cut slopes," Italian J. of Eng. Geol. and Environ., vol. 2, pp. 5–22. 2008.

[7] Ontario, "Trenching Safety," Infrastructure Health & Safety Association. 2017.

[8] F. Mohamed, "A semi-empirical approach for the interpretation of the bearing capacity of unsaturated soils," Master's Thesis, University of Ottawa. 2006.

[9] D. G. Fredlund, and A. Xing, "Equations for the soil-water characteristic curve," *Can. Geotech. J.*, vol. 31, no. 3, pp. 521–532. 1994.

[10] D. G. Fredlund, A. Xing, and S. Huang, "Predicting the permeability function for unsaturated soils using the soil-water characteristic curve," *Can. Geotech. J.*, vol. 31, no. 4, pp. 533–546. 1994.

[11] D. G. Fredlund, and J. Krahn, "Comparison of slope stability methods of analysis," *Can. Geotech. J.*, vol. 14, no 3, pp. 429–439. 1997.

[12] N. R. Morgenstern, and V. E. Price, "The Analysis of the stability of General Slip Surfaces," *Géotechnique*, vol. 15, no. 1, pp. 79–93. 1965.

[13] S. K. Vanapalli, D. G. Fredlund, D. E. Pufahl, and A. W. Clifton, "Model for the prediction of shear strength with respect to soil suction," Can. Geotech. J., vol. 33, pp. 379–392. 1996.

[14] GeoSlope, "Stability modelling with GeoStudio". 2017.